Journal of Earth Sciences and Geotechnical Engineering, vol.7, no. 1, 2017, 215-230
ISSN: 1792-9040 (print version), 1792-9660 (online)
Scienpress Ltd, 2017

The interactions of the Exhaust Ultrafine Particle with the vehicle near-wake flow

Amine Mehel[1], Frederic Murzyn[2] and Romain Rodriguez[2]

Abstract

Reduction of pollution emission coming from automotive engines has become a key strategy leading to some significant improvements in the last two decades in Europe with the implementation of new and tighter regulations. To date, the most important remaining problem concerns the increased emission of ultrafine particles (nanoparticles) especially with the reduction of larger and solid carbonaceous particles. Recent studies have shown that these ultrafine particles (most important in number rather than in mass) are the worst and most harmful particles in terms of health effects. Indeed, they are able to reach the respiratory system in its deepest part, the alveolar region where they can readily penetrate the blood stream leading to major cardiovascular diseases or cancer. Furthermore, it is well-known that these ultrafine particles can infiltrate the vehicle in-cabin and accumulate inside. This enhances the risk exposure of the passengers. In this study, we are not only interested in investigating their dispersion downstream of a reduced-scale square-back car model, but also in studying their interaction with the dynamic of the model near-wake flow turbulence in a wind tunnel. The results show that a high correlation is found between the ultrafine particles dispersion/accumulation zones and the turbulent vortices that are generated in the vehicle near-wake.

Keywords: Aerosol dispersion, Ultrafine Particles, Particle concentration, Turbulence, Wind tunnel, LDV.

1 Introduction

For many decades the particles emissions were not regulated or only limited to the mass concentration. This explains why road traffic has become one of the

[1] Department of Composite Materials Mechanics and Environment, ESTACA, 78180, Montigny-Le-Bretonneux, France
[2] Department of Composite Materials Mechanics and Environment, ESTACA, 53061, Laval, France

major sources of fine and ultrafine particles number concentrations (PNC). Emission measurements campaigns suggest that motor vehicles are the primary direct emission sources of fine and ultrafine particles to the atmosphere in urban areas (Shi et al., 1999; Hitchins et al., 2000; Biswas et al., 2008). They roughly count for 90% or more of the total particle number in areas influenced by on-road vehicles emissions (Morawska et al., 2008). They are in the size range 20–130 nm for diesel engines (Morawska et al., 1998) and 20–60 nm for gasoline engines (Ristovski et al., 1998). The exposure to such ultrafine particles result in causing several adverse health effects. Recent toxicological studies have showed that these ultrafine particles are more toxic than larger particles with the same chemical composition and at the same mass concentration (Brown et al., 2000; Oberdorster, 2001). Indeed, they are able to reach the respiratory system in its deepest part, the alveolar region where they can readily penetrate the blood stream leading to major cardiovascular diseases or cancer (Valberg, 2004; Silverman et al., 2012, Ostro et al., 2015). Thus, the need of particle number concentration (PNC), together with the size distribution (PSD) of ultrafine particles, has led to several studies where measurements have been conducted to better assess ambient air quality and its potential health effects. Among them, Zhu et al. (2002), Janssen et al. (2001), Kozawa et al. (2012) assessed PNC and PSD near major highways and roads. These ultrafine particles are then transported from these regions with very high concentrations to all over the surrounding local environments where they can infiltrate vehicles in-cabin, building, schools and indoor environments. Consequently they can cumulate resulting in the exposure of the passengers, pedestrians, bikers…The exposure to such pollutants has been assessed through local/individual measurements. Particularly, they recent studies have evaluated the individual exposure when commuting in the transportation microenvironment (Adams et al., 2001; Zuurbier et al., 2010), buses or bicycle (Gee & Raper; 1999), vehicles in-cabin (Joodatnia et al., 2013; Zhu et al., 2007). Other investigations have been conducted to compare exposure depending on transport mode (Panis et al., 2010; Knibbs et al., 2011) or during day-time activities including, outdoor commuting in traffic environments (Gu et al. 2015). All these studies have underlined the importance of two major parameters (among others) in assessing the exposure, i.e. the concentration and particle size. This has led some authors to characterize them during different stages of the transportation process. During the infiltration process, it has been shown that parameters such as vehicle mileage, age and ventilation fan speed have strong influence on the indoor to outdoor concentration ratio (Hudda et al., 2012). The pollutants dispersion is also influenced by the local topology as mentioned in Goel & Kumar (2015) or Takano and Moonen (2013). They showed the influence of signalized traffic intersections or of the street canyon roof shape on PNC respectively on pollutants concentration levels.

This brief overview demonstrates the importance of treating particle dynamics at different urban scales as concluded by Kumar et al. (2011). This is the reason why we focus on the dispersion of the UFP in the vehicle wake flow where the

PNC levels are very high and the risk due to exposure elevated. The dispersion process of the UFP at this stage is mostly influenced by the flow and particularly by the turbulent structures. Studying their correlations with PNC would be helpful to identify some key-parameters that may affect particle dispersion. To achieve this goal, we undertake wind tunnel investigations. Across the literature, we notice that only very few experimental studies dealt with that topic (Kanda et al., 2006; Carpentieri et al., 2012). Then, we present new wind tunnel experiments to assess the dynamic of carbonaceous UFP downstream of a reduced-scale truck model. While Carpentieri et al. (2012) used a passive tracer gas, we resort to solid particles. Furthermore, in our experimental conditions, the tailpipe flow and wind tunnel flow mixing are supposed to be representative of an urban vehicle moving at 30km/h (kinematic scale). PNC and velocity field measurements are achieved to bring new understanding regarding UFP interaction with the vehicle near wake flow and its consequence on their dispersion. Results are mostly compared and discussed with Carpentieri et al. (2012). Further perspectives and future works are presented.

2 Experimental method

The present experiments are conducted in two different wind tunnels. The Particle Number Concentrations (PNC) measurements are undertaken in the experimental facility located at ESTACA Paris. The corresponding wind tunnel has a test section of 800mm in length, a width of 600mm and a height of 600mm. The velocity measurements are recorded at ESTACA Laval in the second wind tunnel which is 1m in length, 0.3m in width and 0.3m in height. The same upstream air velocity is ensured and set at U_{mean}=14.4m/s so as to get the same flow conditions in both wind tunnels. This velocity is recorded either with a Pitot tube (Paris) or with a 2D LDV system (Laval). Walls are made of transparent altuglass allowing flow visualization and use of optical devices. The studied car model is shown in Fig. 1 (left). It has a common rear part of a truck with a reduced size. Here, the scale factor is 1/20 compared to a real prototype. The length of the model is L=122mm, its width is W=49mm and its height is H=65mm. For all conditions, the blockage ratio was less than 4%. No raised false floor is installed contrary to Carpentieri et al. (2012) where one was used for some experimental conditions. Nevertheless, a calibration of the wind tunnel is carried out prior to the present experiments to ensure a well-defined knowledge of the undisturbed flow developing in the measurement section. For both wind tunnels, the turbulence intensity of the incoming flow is less than 1%.

Figure 1: Car model used during the experiments (Left) and the Cartesian coordinate system with incoming flow from top left to bottom right (Right)

The experimental conditions are supposed to correspond to a real truck prototype speed U_p=8.33m/s (30km/h) according to an imposed kinematic scale of 1.73 (U_{mean}/U_p). This scale is imposed by some experimental constraints related to the flow rate of the exhausted particles. Hence, the dynamic similarity of the tailpipe jet and wind tunnel air flows is ensured. The associated Reynolds number based on the truck height and kinematic viscosity of air is 6.10^5 ($Re=U_{mean}*H/\nu=6.10^5$). This is significantly larger than critical value of 10^4 from which the boundary layer at the rear of the car becomes turbulent. According to Hucho (1998), above this limit, little sensitivity to the Reynolds number is expected. During the experiments, the kinematic scale between prototype and model is kept constant for exhausted gas/particle velocity considering a given engine speed of 2500 rpm. It is worthwhile to note that this condition is a novelty in comparison to the previous studies on pollutant dispersion in wind tunnels. The nanoparticles are generated by a PALAS DNP 2000 spark discharge aerosol generator using graphite electrodes and Nitrogen. The aerosol is injected in the model tailpipe at a given flow rate of Q_{cp}=0.133L/s. The size distribution of ultrafine carbon particles ranges from 20 to 100nm. An Electrical Low Pressure Impactor (ELPI) is used for Particle Number Concentration (PNC) measurements. Altogether these experimental conditions are supposed to be typical of urban areas. Additional details dealing with experimental conditions are given by Mehel and Murzyn (2015).

The Particle Number Concentrations are measured at 66 different locations downstream of the car corresponding to distinct positions in the longitudinal (x), vertical (y) and transversal (z) directions. Altogether they cover a domain given by $0.25<X=x/H<5$, $0.25<Y=y/H<1$ and $-0.5<Z=z/H<0.5$ where H is the height of the truck. This finite volume is imposed by the size of the wind tunnel section. Therefore, according to the dimensions of the experimental facilities, we are mostly focused on the near-wake region ($x/H<5$). For completeness, the origin of the axis system (Fig. 1, right) is taken on the centerline of the wind tunnel (z=0), on the ground (y=0) and on the rear face of the car model (x=0). In the dimensionless coordinate system, the injection point representing the tailpipe is

located at X=x/H=0, Y=y/H=0.25 and z/H=-0.25.

For PNC measurements, data acquisition lasts 120 seconds and the data rate is kept constant and equal to 1 Hertz. The acquisition duration is long enough compared to the time scale of the flow. So the convergence of the concentration data is ensured.

The velocity fields are measured using a 2D LDV system (DANTEC) mounted on a 2D displacement table. Both streamwise (U) and vertical (V) components of the velocity are recorded at 560 different locations downstream of the truck. The corresponding investigated area spreads such as $0.25<X<5$, $0.25<Y<1$ and $\sim -0.55<Z<0$. The measurement grid consists of 20 x 7 x 4 points. On the x-axis, the step between 2 points is 16.25mm while it is 8.25mm on the y-axis and 12mm on the z-axis. Data acquisition lasts 60 seconds or ends as soon as 5000 samples are acquired. To avoid any erroneous measurements, velocity data are filtered based on the rms value of U and V. That is, if $U-U_{mean}$ (or $V-V_{mean)}$ is larger than 3u' (3v' respectively) where u' and v' are the rms values of U and V, then the pair (U, V) is replaced by (U_{mean}, V_{mean}). This filtering technique only concerns few points (less than 1%) and does not significantly affect U_{mean}, V_{mean}, u' and v' (Murzyn and Belorgey, 2005). Furthermore, measured points where data rate is below 5Hz are systematically removed as they may not represent the real flow dynamic where rapid fluctuations occur. Nevertheless, this only represents a very low number of points (less than 2%) and may be explained by possible invisible scratches on the wind tunnel walls for instance.

For all measurements, we acknowledge a constant air speed (steady conditions) and no heat flux from engine is considered. Lastly, it should be noticed that even if the aerosol is not heated, the particles are less sensitive to the buoyancy effect than if a gaseous passive tracer was used. Indeed, their density is approximately $2000 kg/m^3$ (carbon particle). This point is a main difference compared to the experimental investigations of Kanda et al. (2006) and Carpentieri et al. (2012) where a gas tracer was used.

3 Results and Discussion

For the following figures, black marks indicate the measurement positions. An absence of symbol means unavailable data due to data rate below 5Hz and/or possible scratch on the side of the wind tunnel.

Mean velocity fields

Figure 2 presents a 2D vertical map (xy) of the dimensionless mean streamwise velocity (U/U_{mean}) measured at the centreline of the channel (z/H=0). Our results indicate that a negative streamwise velocity component is found close to the rear of the vehicle (x/H<1) over a height which approximately corresponds to 0.80H. The minimum streamwise velocity (U~-0.23m/s) is found at x/H=0.5 and

y/H~0.38. Overall, this finding is in accordance with results from Carpentieri et al. (2012). Out of this very near-wake region, positive streamwise velocities are measured with increasing values when the distance to the vehicle increases. This characterizes a recirculating flow that appears in the near-wake of the vehicle Ahmed et al (1984). From the present measurements, the length of this region is estimated at approximately 1H when Carpentieri et al. (2012) suggested 2H. This is not in contradiction as they did not strictly use the same shape for the vehicle model. Far downstream (top right of figure 2), the flow recovers the same mean streamwise velocity as upstream (U/U_{mean}~1) for x/H>4 and y/H>0.90. The transition between the recirculation and the "far wake" regions is gradual. This is also in agreement with Carpentieri et al. (2012).

Figure 3 presents the same 2D vertical map for the dimensionless mean vertical velocity (V/U_{mean}) measured at the centreline of the channel (z/H=0). For 0<x/H=0.75 and y/H up to 0.90, positive values are found depicting an upward mean flow motion. Similarly, at x/H=0.50, an upward motion occurs up to y/H~0.50. Everywhere else, negative values are encountered. For x/H>0.75, dimensionless values are between -0.20 and -0.05 (-2.90m/s and -0.7m/s). Far downstream (x/H=5), the dimensionless vertical component of the velocity is roughly homogeneous with an average value of -0.05. The flow is back to a quasi 1D structure similar to the upstream conditions. Combining with the above results, this clearly denotes the apparition of recirculation vortex in the vicinity of the car model. From the mean velocity field, we put in evidence its development close to the car model. This is in accordance with past results (Carpentieri et al., 2012). The structure and the dynamic of the flow in this near-wake region are of importance and have significant impact on the PNC measurements as it will be seen in the next section.

For completeness, Figs 4 and 5 present the same characteristics relative to the mean flow but for a different 2D cross section. Here, the (yz) map is considered at x/H=0.50 (near-wake). It only represents half of the symmetrical near-wake flow. Taking into account the width of the car model, it is worthwhile to note that the lateral sides of the car are situated at z/H~+/-0.38. From these figures, some relevant information can be deduced. From the lower vertical position y/H=0.25 to y/H~0.75, negative horizontal streamwise velocities are encountered when z/H<0.20. In the same time, vertical component of the velocity vector is mostly positive when y/H<0.50 whatever z/H is. It is believed that the recirculation area may be symmetrical but does not spread over the whole width of the vehicle. Out of this very near-wake region (for (x/H>2), our results show that horizontal streamwise velocity is always positive. This is also true at x/H=1 except for the position y/H=0.25 and z/H=0 where a negative horizontal streamwise velocity is recorded. This reveals that the recirculation region is limited to the closest vicinity of the car model.

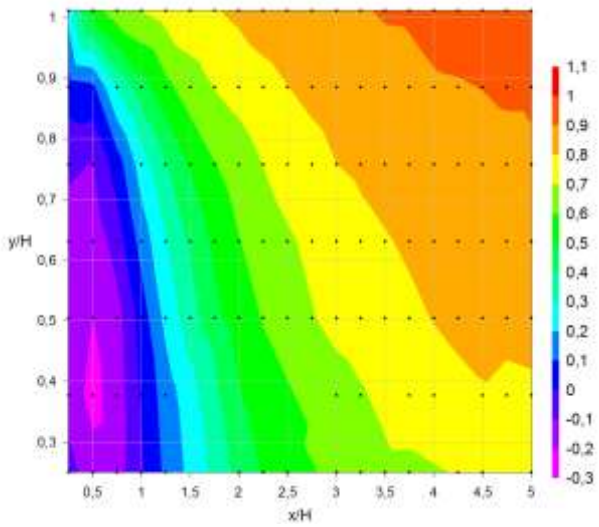

Figure 2: 2D map (xy) of dimensionless mean streamwise velocity (z/H=0)

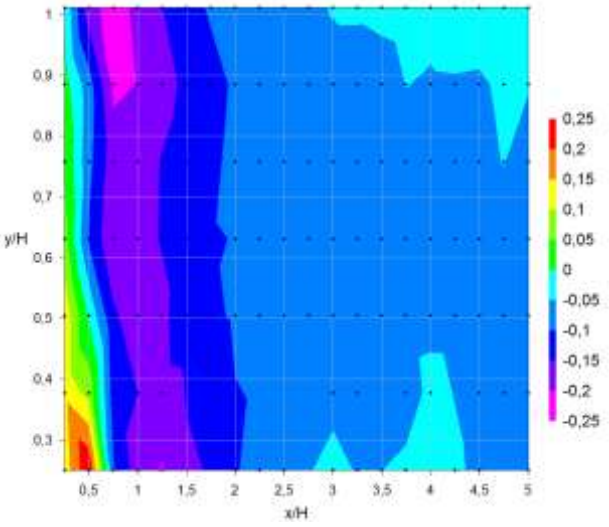

Figure 3: 2D map (xy) of dimensionless mean vertical velocity (z/H=0)

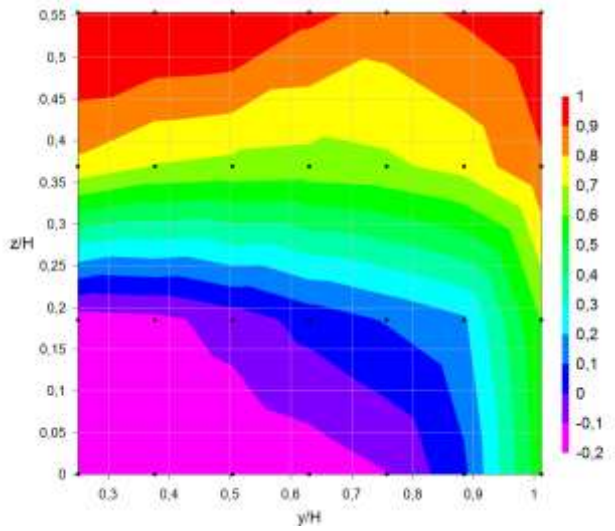

Figure 4: 2D map (yz) of dimensionless mean streamwise velocity (x/H=0.50)

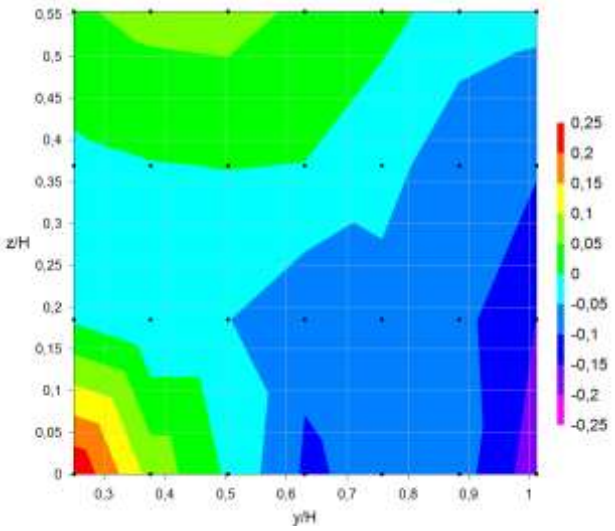

Figure 5: 2D map (yz) of dimensionless mean vertical velocity (x/H=0.50)

Turbulent velocity fields

Figures 6 and 7 present the turbulence intensity in both longitudinal (Ix) and vertical (Iy) directions respectively. Ix and Iy are expressed as the ratio between rms of the corresponding velocity component and Umean. The displayed data correspond to the centreline of the wind tunnel (z/H=0). Note that the scale is kept identical to make the comparison easier.

For the given transverse position z/H=0, our results for the turbulence intensity levels (Figs 6 and 7) exhibit that the turbulence level is overall more intense close to the vehicle and decreases with the dimensionless distance x/H. Except for one position (x/H=0.50 and y/H=0.25 where Ix reaches 25.5%) the turbulence intensity does not exceed 17%. Peaks are mainly measured at heights corresponding to upper (0.80<y/H<1) and lower (y/H<0.40) surfaces of the car model. This behaviour was previously observed by Carpentieri et al. (2012) within a comparable range. Furthermore, a similar behaviour is highlighted. Indeed, at the roof height (y/H~1), we found the highest turbulence level at x/H=0.75 (Ix=16.8%). Close to the ground, the maximum is measured at x/H=0.50 (Ix=25.5%). This longitudinal gap between both peaks has been reported by Carpentieri et al. (2012) as well. Regarding Iy (Fig. 7), the highest level is estimated slightly below 20% but average results are pretty much the same as I_x (Fig. 6).

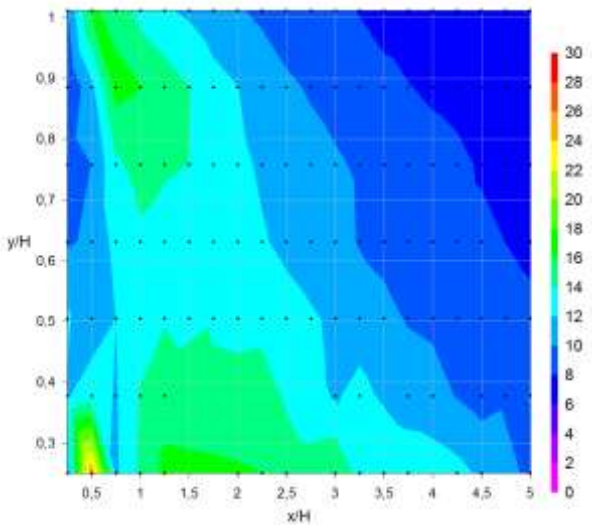

Figure 6: 2D map (xy) of turbulence intensity Ix (z/H=0)

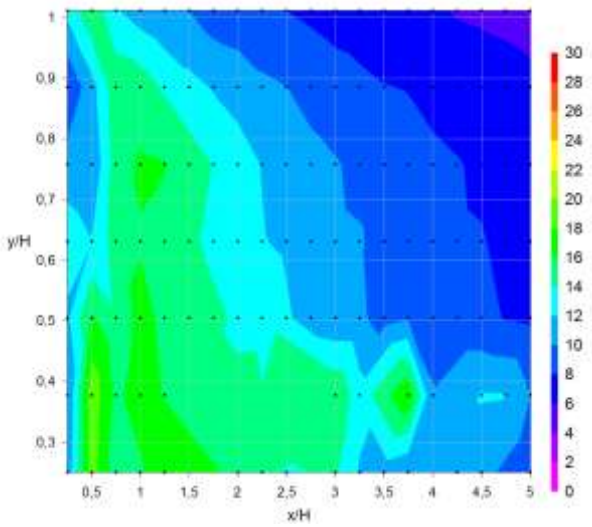

Figure 7: 2D map (xy) of turbulence intensity Iy (z/H=0)

Far downstream, both average levels of turbulence (I_x and I_y) fall below 10%. The wake is still disturbed compared to the upstream flow conditions and a larger distance is required to get back to the upstream flow conditions.

Particle Number Concentration (PNC)

Two different 2D maps of Particle Number Concentrations are presented on Figs 8 and 9.

Figure 8 corresponds to a vertical section at the centreline of the channel (z/H=0). It shows that the most important PNC (PNC>2.10^6) is observed in the vicinity of the car (x/H<1). This is not surprising since it corresponds to the emission point region. The maximum PNC reaches $3.38.10^6$ for x/H=0.50 and y/H=0.25 (height of the tailpipe). In the spanwise direction (vehicle width), the PNC evolves according to a particular behaviour: close to the vehicle (x/H<1), nanoparticles are entrapped by the recirculation cell leading to highest concentrations in the centreline at z/H=0. By looking at these PNC contours for z/H=-0.30 (approximated position of the tailpipe), the maximum of PNC is found between x/H=0.50 and 1 for y/H=0.25. The corresponding levels are $1.21.10^6$ (x/H=0.50 and y/H=0.25) and $1.29.10^6$ (x/H=1 and y/H=0.25). For z/H=-0.50 and 0.50 (outer of the vehicle width), peaks are mostly found from x/H=5 rather than in the very near wake region (x/H<1).

This is strongly related to the near wake flow structure pointed out from the velocity measurements. At z/H=0, nanoparticles are sucked by this large recirculating structure and accumulate in this part of the flow. It has an approximated size of 0.50 to 1H in length and 0.50 to 0.80H in height. Once the nanoparticles are trapped by the large recirculating vortex, the mechanism of turbulence diffusion takes place driving them to the area where I_x and I_y are lower

which corresponds to x/H<0.75 and y/H>0.5 as noticed above (Figs 6 and 7). As a result, the plume is enhanced in the vertical direction. The highest PNC correspond to highest levels of I_y. Interaction between turbulence and particles is then obvious. This behaviour was previously mentioned by Mehel and Murzyn (2015) and illustrates the strong influence of the vehicle wake on the development of the plume.

In the cross-section at x/H=1 (Fig. 9), the cloud of dispersed nanoparticles enlarges and spreads in the spanwise direction. At x/H=1, the shape of the plume is roughly Gaussian but not centred around z/H=0. Far downstream (x/H=2 to 5), we show that a clear dissymmetry appears and the most important PNC are found between z/H=-0.50 and -0.30 (Fig. 10). This clearly denotes that the dynamic of the nanoparticles is strongly influenced by the pair of lateral longitudinal outer vortices that develop and propagate from both edges of the car. The highest number of particles is also found in the lower part of the flow (y/H<0.50) which corresponds to the position of the tailpipe. For x/H=0.50, 1, 2 and 5, the highest PNC values are $3.38.10^6$ (y/H=0.25 and z/H=0), $1.29.10^6$ (y/H=0.25 and z/H=-0.30), $0.548.10^6$ (y/H=0.25 and z/H=-0.30), $0.293.10^5$ (y/H=0.25 and z/H=-0.30). Therefore, the decay rate is inversely proportional to the dimensionless distance to the car model and is related to the dilution process.

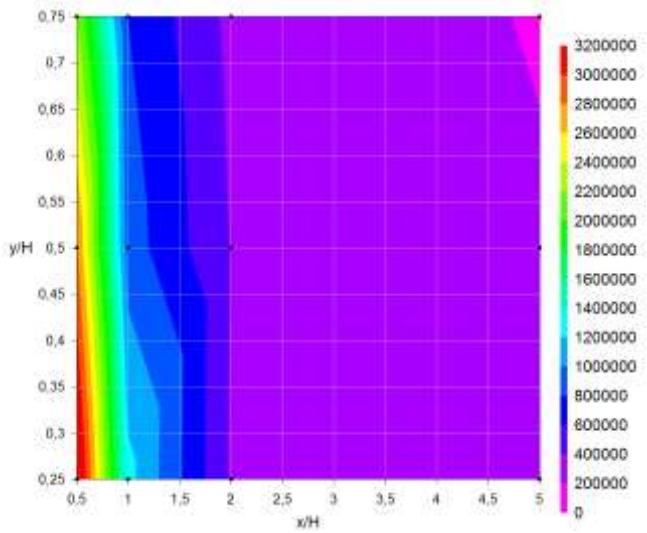

Figure 8: 2D map (xy) of PNC (z/H=0)

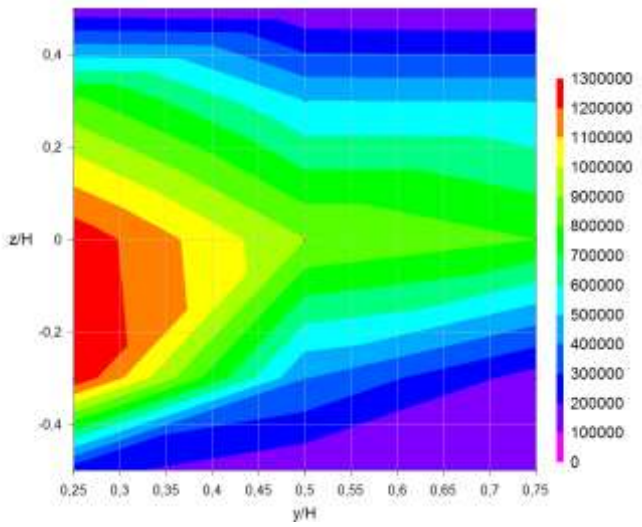

Figure 9: 2D map (yz) of PNC (x/H=1)

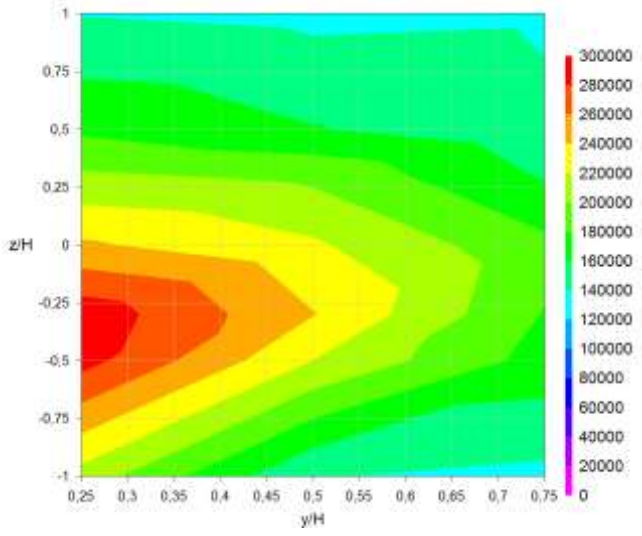

Figure 10: 2D map (yz) of PNC (x/H=5)

At the same time, at x/H=0.50, the maximum PNC is found at z/H=0 while it is shifted to z/H=-0.30 for x/H=1, 2 and 5. It is worthwhile to note that z/H=-0.30 roughly corresponds to the position of the lateral side of the car model and the tailpipe position. For x/H=1, a second peak close to the first one (PNC=$1.27.10^6$) is measured showing that lateral dispersion really starts downstream of x/H=1. According to the literature, this is also related to lateral vortices that develop in this region from the edge of the car (Hucho, 1998). Our results confirm that the vortices appearing in the near wake flow strongly influence the dispersion of the emitted particles. Accordingly, the turbulence plays an important role in the

dispersion of nanoparticles emitted from the tailpipe of a car and the development of the corresponding plume.

4 Conclusion

In the present paper, we present experimental results of wind tunnel investigations regarding the correlation between flow dynamic and Particle Number Concentration in the wake of a vehicle model. Prior to this contribution, only few studies have been undertaken to assess this link. Here, we measure the mean and turbulent properties of the near-wake flow developing downstream of a passenger car and the Particle Number Concentration (PNC). The experimental flow conditions are defined so as to be representative of a real car at 30km/h (urban cycle) according to a kinematic scale. The flow developing downstream of the car is characterized using a 2D LDV system and a grid of 560 points is defined for velocity measurements while PNC are recorded at 66 locations. Although we acknowledge that some improvements may be brought by reducing the step between 2 measurement points, by exploring the 3D flow or by considering more accurately the boundary layer effect, it is also expected that these preliminary results will be helpful for the community. From the measurements, our main conclusions highlight that:

- A recirculating flow develops in the close vicinity of the car model which size is estimated and compared with the previous work of Carpentieri et al. (2012) showing interesting consistency;
- The longitudinal and vertical turbulence intensities are investigated showing peaks around 25% and 20% for I_x and I_y respectively;
- Two main regions of intense turbulence activity are revealed either at the roof level or close to the ground with a longitudinal gap;
- PNC measurements in the near-wake depict a strong influence of the recirculation region which is able to suck particles leading to highest concentrations at the centreline of the channel for lowest values x/H. Then they are diffused in the vertical direction towards low level of turbulence intensities I_x and I_y;
- When increasing the distance to the vehicle, our results indicate that lateral vortices developing from the edge of the car are capable of trapping particles. This is put in evidence by looking at the off-centre distribution of PNC. Far downstream, the peak of PNC is found to be in-line with the tailpipe. This point is important for numerical modelling as the position of the tailpipe must be taken into account with accuracy.

Altogether, these results are an added value to the existing literature and supplement interestingly some preliminary PNC measurements published earlier (2015). They particularly show the narrow relation existing between flow turbulence dynamics and particle dispersion. Nevertheless, the remaining questions are still numerous. As a consequence, some further experimental measurements and in-situ campaigns will be

scheduled in the context of two new PhD research project startings focusing on correlation between wake flow and PNC.

References

[1] Adams, H. S., Nieuwenhuijsen, M. J., Colvile, R. N., McMullen, M. A. S., & Khandelwal, P. (2001). Fine particle (PM 2.5) personal exposure levels in transport microenvironments, London, UK. Science of the Total Environment, 279(1), 29-44.

[2] Ahmed, S. R., Ramm, G., & Faitin, G. (1984). Some salient features of the time-averaged ground vehicle wake (No. SAE-TP-840300). Society of Automotive Engineers, Inc., Warrendale, PA.

[3] Brown, D. M., Stone, V., Findlay, P., MacNee, W., & Donaldson, K. (2000). Increased inflammation and intracellular calcium caused by ultrafine carbon black is independent of transition metals or other soluble components. Occupational and Environmental Medicine, 57(10), 685-691.

[4] Carpentieri, M., Kumar, P., & Robins, A. (2012). Wind tunnel measurements for dispersion modelling of vehicle wakes. Atmospheric environment, 62, 9-25.

[5] Janssen, N. A., van Vliet, P. H., Aarts, F., Harssema, H., & Brunekreef, B. (2001). Assessment of exposure to traffic related air pollution of children attending schools near motorways. Atmospheric environment, 35(22), 3875-3884.

[6] Joodatnia, P., Kumar, P., & Robins, A. (2013). The behaviour of traffic produced nanoparticles in a car cabin and resulting exposure rates. Atmospheric environment, 65, 40-51.

[7] Gee, I. L., & Raper, D. W. (1999). Commuter exposure to respirable particles inside buses and by bicycle. Science of the Total Environment, 235(1), 403-405.

[8] Goel, A., & Kumar, P. (2015). Zone of influence for particle number concentrations at signalised traffic intersections. Atmospheric Environment, 123, 25-38.

[9] Gu, J., Kraus, U., Schneider, A., Hampel, R., Pitz, M., Breitner, S., ... & Cyrys, J. (2015). Personal day-time exposure to ultrafine particles in different microenvironments. International journal of hygiene and environmental health, 218(2), 188-195.

[10] Hitchins, J., Morawska, L., Wolff, R., Gilbert, D., (2000). Concentrations of submicrometer particles from vehicle emissions near a major road. Atmospheric Environment 34, 51–59.

[11] Hucho W.H. (1998), Aerodynamics of road vehicles: From fluid mechanics to vehicle engineering, Society of Automotive Engineering.

[12] Kanda, I., Uehara, K., Yamao, Y., Yoshikawa, Y., & Morikawa, T. (2006). A wind-tunnel study on exhaust gas dispersion from road vehicles—Part I: Velocity and concentration fields behind single vehicles. Journal of wind engineering and industrial aerodynamics, 94(9), 639-658.

[13] Knibbs, L. D., Cole-Hunter, T., & Morawska, L. (2011). A review of commuter exposure to ultrafine particles and its health effects. Atmospheric Environment, 45(16), 2611-2622.

[14] Kozawa, K. H., Winer, A. M., & Fruin, S. A. (2012). Ultrafine particle size distributions near freeways: Effects of differing wind directions on exposure. Atmospheric Environment (Oxford, England : 1994), 63, 250–260.

[15] Kumar, P., Ketzel, M., Vardoulakis, S., Pirjola, L., & Britter, R. (2011). Dynamics and dispersion modelling of nanoparticles from road traffic in the urban atmospheric environment—a review. Journal of Aerosol Science, 42(9), 580-603.

[16] Mehel, A., & Murzyn, F. (2015). Effect of air velocity on nanoparticles dispersion in the wake of a vehicle model: Wind tunnel experiments. Atmospheric Pollution Research, 6(4), 612-617.

[17] Morawska, L., Ristovski, Z., Jayaratne, E.R., Keogh, D.U., Ling, X. (2008). Ambient nano and ultrafine particles from motor vehicle emissions: characteristics, ambient processing and implications on human exposure. Atmospheric Environment 42, 8113-8138.

[18] Morawska, L., Bofinger, N.D., Kocis, L., Nwankwoala, A., (1998). Submicrometer and super micrometer particles from diesel vehicle emissions. Environmental Science and Technology 32, 2033–2042.

[19] Murzyn, F. and Belorgey, M. (2005). Experimental investigations of the grid-generated turbulence features in a free-surface flow, Experimental Thermal and Fluid Science, 29, pp925-935.

[20] Oberdorster, G., (2001). Pulmonary effects of inhaled ultrafine particles. International Archives of Occupational and Environmental Health 74 (1), 1–8.

[21] Ostro B, Hu J, Goldberg D, Reynolds P, Hertz A, Bernstein L, Kleeman MJ. 2015. Associations of mortality with long-term exposures to fine and ultrafine particles, species and sources: results from the California Teachers Study cohort. Environ Health Perspect 123:549–556

[22] Panis, L. I., De Geus, B., Vandenbulcke, G., Willems, H., Degraeuwe, B., Bleux, N., & Meeusen, R. (2010). Exposure to particulate matter in traffic: a comparison of cyclists and car passengers. Atmospheric Environment, 44(19), 2263-2270.

[23] Ristovski, Z.D., Morawska, L., Bofinger, N.D., Hitchins, J., (1998). Submicrometer and supermicrometer particles from spark ignition vehicles. Environmental Science and Technology 32, 3845–3852.

[24] Shi, J.P., Khan, A.A., Harrison, R.M., (1999). Measurements of ultrafine particle concentration and size distribution in the urban atmosphere. Science of the Total Environment 235, 51–64.

[25] Takano, Y., & Moonen, P. (2013). On the influence of roof shape on flow and dispersion in an urban street canyon. Journal of Wind Engineering and Industrial Aerodynamics, 123, 107-120.
[26] Zhu, Y.; Hinds, W.C., Kim, S., Shen, S. & Sioutas, C., (2002). Study of ultrafine particles near a major highway with heavy-duty diesel traffic, Atmospheric Environment, Volume 36, Issue 27, Pages 4323-4335.
[27] Zhu, Y., Eiguren-Fernandez, A., Hinds, W. C., & Miguel, A. H. (2007). In-cabin commuter exposure to ultrafine particles on Los Angeles freeways. Environmental science & technology, 41(7), 2138-2145.
[28] Zuurbier, M., Hoek, G., Oldenwening, M., Lenters, V., Meliefste, K., van den Hazel, P., & Brunekreef, B. (2010). Commuters' exposure to particulate matter air pollution is affected by mode of transport, fuel type, and route. Environmental health perspectives, 118(6), 783.

.